

Search for Heavy Neutral Leptons with IceCube DeepCore

Dissertation
zur Erlangung des akademischen Grades
doctor rerum naturalium
(Dr. rer. nat.)

im Fach: Physik
Spezialisierung: Experimentalphysik

eingereicht an der
Mathematisch-Naturwissenschaftlichen Fakultät
der Humboldt-Universität zu Berlin

von
Leander Fischer M. Sc.
geboren am 24. Oktober 1992
in Heidelberg

Präsidentin der Humboldt-Universität zu Berlin
Prof. Dr. Julia von Blumenthal

Dekanin der Mathematisch-Naturwissenschaftlichen Fakultät
Prof. Dr. Caren Tischendorf

Copyright Notice

This book is released into the public domain using the CC-BY-4.0 code.

To view a copy of the CC-BY-4.0 code, visit:

<https://creativecommons.org/licenses/by/4.0/>

Colophon

This document was typeset with the help of KOMA-Script and L^AT_EX using the open-source kaobook template class.

The source code of this thesis is available at:

https://github.com/LeanderFischer/phd_thesis

Zusammenfassung

Zusammenfassung ...

Abstract

Abstract ...

Todo list

adjust final vertical position of this reference	1
Also cite this? Didn't find a good reference, only the press releases.	1
Introduce SM EW NC/CC Lagrangian to build upon in the next chapter	3
Plot is missing + for W and 0 for Z boson.	3
Cite and/or sidenote this.	4
cite this	4
cite neutrino oscillations/flavor conversions	4
namedrop RH=sterile=HNL and why they are called like this based on the SM EW Lagrangian introduced above	4
write some interlude to motivate atm. neutrinos as source for HNL searches/production etc.	6
Say something about atmospheric neutrino flux uncertainties, based on recent JP/Anatoli papers.	7
add current BF values from nufit or so?	9
say something about how this changes with matter	10
Re-write/re-formulate this section (copied from HNL technote).	10
Produce similar styled plot for these limits	10
This section really needs to be re-written to motivate the search for HNLs from a more generic point of view (e.g. to explain neutrino masses)	11
This section definitely needs to be elaborated in a little more detail	11
Not adding information about the case where the neutrinos have Dirac or pseudo-Dirac masses	12
describe the "good fit" selection	16
add information about the matter profile used	21
add information about the oscillation probability calculation and the software used for it	21
Should I adapt the total numbers to match the sum of the rounded individual parts?	21
add 3D expectation and/or S/sqrt(B) plots	22
Add fractions of the different particle types in the bins for benchmark mass/mixing (another table?) .	22
Do I want/need to include the description of the KDE muon estimation?	23
Add table with all systematic uncertainties used in this analysis.	23
add final level effects of varying the axial mass parameters (or example of one)	23
add final level effects of varying the DIS parameter (or example of one)	23
Do I want additional plots for this (fit diff, LLH distr, minim. stats, param. fits)?	24
Add bin-wise TS distribution? Add 3D TS maps?	25
Add table with BFP mixings and their uncertainties from scan assuming wilks?	25
Add table with BFP nuisance parameters and maybe a plot showing them compared to nominal?	25

Re-make plot with x,y for horizontal set one plot!	29
Re-make plot with x, y, z for both cascades in one.	29
Re-arrange plots in a more sensible way.	29

Contents

Abstract	iii
Contents	vii
1 Standard Model Neutrinos and Beyond	1
1.1 The Standard Model	1
1.1.1 Fundamental Fields	1
1.1.2 Electroweak Symmetry Breaking	2
1.1.3 Fermion Masses	3
1.1.4 Weak Interactions after Symmetry-Breaking	3
1.2 Beyond the Standard Model	3
1.2.1 Mass Mechanisms	4
1.2.2 Observational Avenues for Right-Handed Neutrinos	5
1.2.3 Searching for Heavy Neutral Leptons	6
1.3 Atmospheric Neutrinos as Source of Heavy Neutral Leptons	6
1.3.1 Production of Neutrinos in the Atmosphere	6
1.3.2 Interactions with Nuclei	7
1.3.3 Oscillations	8
1.3.4 Testing Heavy Neutral Leptons with Atmospheric Neutrinos	10
2 Detecting Low Energetic Double Cascades	15
2.1 Reconstruction	15
2.1.1 Table-Based Minimum Likelihood Algorithms	15
2.1.2 Double Cascade Hypothesis	15
2.1.3 Modification to Low Energy Events	15
2.2 Cross Checks	15
2.2.1 Simplistic Sets	15
2.3 Performance	16
2.3.1 Energy/Decay Length Resolution	16
2.3.2 Double Cascade Classification	18
3 Search for an Excess of Heavy Neutral Lepton Events	21
3.1 Final Level Sample	21
3.1.1 Expected Rates/Events	21
3.1.2 Analysis Binning	22
3.2 Statistical Analysis	23
3.2.1 Low Energy Analysis Framework	23
3.2.2 Test Statistic	23
3.2.3 Systematic Uncertainties	23
3.3 Analysis Checks	23
3.3.1 Minimization Robustness	24
3.3.2 Ensemble Tests	24
3.4 Results	25
3.4.1 Best Fit Parameters	25
3.4.2 Upper Limits	25
3.4.3 Post-Fit Data/MC Agreement	25
3.4.4 Likelihood Coverage	25

APPENDIX	27
A Heavy Neutral Lepton Signal Simulation	29
A.1 Model Independent Simulation Distributions	29
A.2 Model Dependent Simulation Distributions	30
B Analysis Checks	31
B.1 Minimization Robustness	31
B.1.1 Ensemble Tests	31
Bibliography	33

List of Figures

1.1	Feynman diagrams of neutrino weak interactions	3
1.2	HNL decay widths	6
1.3	Atmospheric neutrino fluxes	7
1.4	Neutrino-nucleon deep inelastic scattering	8
1.5	Total inclusive neutrino-nucleon cross-sections	9
1.6	Current $ U_{\tau 4}^2 - m_4$ limits	11
1.7	Feynman diagram of HNL up-scattering process	13
1.8	Feynman diagram of HNL decay	13
1.9	HNL branching ratios	13
3.1	Asimov inject/recover test (0.6 GeV)	24
3.2	Pseudo-data trials TS distribution (0.6 GeV)	25
A.1	Simplified model independent simulation generation level distributions	29
A.2	Realistic model independent simulation generation level distributions	30
A.3	Model dependent simulation generation level distributions	30
B.1	Asimov inject/recover test (0.3 GeV, 1.0 GeV)	31
B.2	Pseudo-data trials TS distribution (0.3 GeV, 1.0 GeV)	31

List of Tables

1.1	Standard model fermions	2
3.1	Final level background event/rate expectation	21
3.2	Final level signal event/rate expectation	22
3.3	Analysis binning	22
3.4	Staged minimization routine settings	24

Standard Model Neutrinos and Beyond

1

1.1 The Standard Model

The *Standard Model (SM)* of particle physics is a Yang-Mills theory [1] providing very accurate predictions of weak, strong, and *electromagnetic (EM)* interactions. It is a relativistic quantum field theory that relies on gauge invariance, where all matter is made up of fermions, which are divided into quarks and leptons, and bosons describe the interactions between the fermions that have to fulfil the overall symmetry of the theory. Leptons are excitations of Dirac-type fermion fields.

The initial idea of the theory is associated with the works of Weinberg [2], Glashow [3], and Salam [4], that proposed a unified description of EM and weak interactions as a theory of a spontaneously broken $SU(2) \times U(1)$ symmetry for leptons, predicting a neutral massive vector boson Z^0 , a massive charged vector boson W^\pm , and a massless photon γ as the gauge bosons. The Higgs mechanism [5], describing the breaking of the symmetry, predicts the existence of an additional scalar particle, the Higgs boson, giving the W^\pm and Z^0 bosons their mass. The Higgs boson was discovered in 2012 at the LHC.

Gell-Mann and Zweig proposed the quark model in 1964 [6, 7], which was completed by the discovery of non-abelian gauge theories [8] to form the $SU(3)$ symmetry of the strong interaction called *quantum chromodynamics (QCD)*. QCD describes the interaction between quarks and gluons which completed the full picture of the SM in the mid-1970s. Together with the electroweak theory, the SM is a $SU(3)_C \times SU(2)_L \times U(1)_Y$ local gauge symmetry, with the conserved quantities C , *color*, L , *left-handed chirality*, and Y , *weak hypercharge*.

In the following, the basic properties of the SM are described, following the derivations of [9, 10].

1.1.1 Fundamental Fields

Fermions in the SM are Weyl fields with either *left-handed (LH)* or *right-handed (RH)* chirality, meaning they are eigenvectors of the chirality operator γ_5 with $\gamma_5 \psi_{R/L} = \pm \psi_{R/L}$. Only LH particles transform under $SU(2)_L$. The Higgs field is a complex scalar field, a doublet of $SU(2)_L$, which is responsible for the spontaneous symmetry breaking of $SU(2)_L \times U(1)_Y$ to $U(1)_{\text{EM}}$. Local gauge transformations of the fields are given by

$$\psi \rightarrow e^{ig\theta^a(x)T^a} \psi , \quad (1.1)$$

where g is the coupling constant, $\theta^a(x)$ are the parameters of the transformation, and T^a are the generators of the group, with a counting them. The number of bosons is dependent on the generators of the symmetry groups, while the strength is defined by the coupling constants. There are eight massless gluons corresponding to the generators of the $SU(3)_C$

1.1 The Standard Model	1
1.2 Beyond the Standard Model	3
1.3 Atmospheric Neutrinos as adjust final vertical position source of Heavy Neutral leptons reference	6

[1]: Yang et al. (1954), "Conservation of Isotopic Spin and Isotopic Gauge Invariance"

[2]: Weinberg (1967), "A Model of Leptons"

[3]: Glashow (1961), "Partial-symmetries of weak interactions"

[5]: Higgs (1964), "Broken symmetries, massless particles and gauge fields"

Also cite this? Didn't find a good reference, only the press releases.

[6]: Gell-Mann (1964), "A Schematic Model of Baryons and Mesons"

[7]: Zweig (1964), "An $SU(3)$ model for strong interaction symmetry and its breaking. Version 2"

[9]: Giunti et al. (2007), *Fundamentals of Neutrino Physics and Astrophysics*

[10]: Schwartz (2013), *Quantum Field Theory and the Standard Model*

group. These mediate the strong force which conserves color charge. The W_1, W_2, W_3 , and B boson fields of the $SU(2)_L \times U(1)_Y$ group are mixed into the massive bosons through spontaneous symmetry breaking as

$$W^\pm = \frac{1}{\sqrt{2}}(W_1 \mp iW_2) \quad (1.2)$$

and

$$Z^0 = \cos \theta_W W_3 - \sin \theta_W B, \quad (1.3)$$

with θ_W being the *Weinberg angle*. The massless photon field is given by

$$A = \sin \theta_W W_3 + \cos \theta_W B \quad (1.4)$$

and its conserved quantity is the EM charge Q , which depends on the weak hypercharge, Y , and the third component of the weak isospin, T_3 , as $Q = T_3 + Y/2$.

	Type			Q
quarks	u	c	t	+2/3
	d	s	b	-1/3
leptons	ν_e	ν_μ	ν_τ	0
	e	μ	τ	-1

Table 1.1: Fermions in the Standard Model. Shown are all three generations of quarks and leptons with their electric charge Q .

Fermions are divided into six quarks and six leptons. Weak, strong, and EM force act on the quarks, and they are always found in bound form as baryons or mesons. Leptons do not participate in the strong interaction and only the electrically charged leptons are massive and are effected by the EM force, while neutrinos are massless and only interact via the weak force. Each charged lepton has an associated neutrino, which it interacts with in *charged-current (CC)* weak interactions, that will be explained in more detail in Section 1.1.4. The fermions are listed in Table 1.1.

1.1.2 Electroweak Symmetry Breaking

To elaborate the process of spontaneous symmetry breaking through which the gauge bosons of the weak interaction acquire their masses, the Lagrangian of the Higgs field is considered as

$$\mathcal{L}_{\text{Higgs}} = (D_\mu \Phi^\dagger)(D^\mu \Phi) - \lambda \left(\Phi^\dagger \Phi - \frac{v^2}{2} \right)^2, \quad (1.5)$$

with parameters λ and v , where λ is assumed to be positive. Φ is the Higgs doublet, which is defined as

$$\Phi = \begin{pmatrix} \Phi^+ \\ \Phi^0 \end{pmatrix}, \quad (1.6)$$

with the charged component Φ^+ and the neutral component Φ^0 . The covariant derivative is given by

$$D_\mu = \partial_\mu - ig_2 \frac{\sigma^i}{2} W_\mu^i - \frac{1}{2}ig_1 B_\mu, \quad (1.7)$$

with the Pauli matrices σ^i and the gauge boson fields W_μ^i and B_μ of the $SU(2)_L$ and $U(1)_Y$ groups, respectively. The coupling constants g_2 and g_1 are the respective coupling constants which are related to the Weinberg angle as $\tan \theta_W = \frac{g_1}{g_2}$. The Higgs potential has a non-zero *vacuum expectation value (vev)* at the minimum of the potential at $\Phi^\dagger \Phi = \frac{v^2}{2}$. Since the vacuum is electrically neutral, it can only come from a neutral

component of the Higgs doublet as

$$\Phi_{\text{vev}} = \frac{1}{\sqrt{2}} \begin{pmatrix} 0 \\ v \end{pmatrix}. \quad (1.8)$$

1.1.3 Fermion Masses

The mass term for charged fermions with spin-1/2 is given by

$$\mathcal{L}_{\text{Dirac}} = m(\bar{\Psi}_R \Psi_L - \bar{\Psi}_L \Psi_R), \quad (1.9)$$

composed of the product of left- and RH Weyl spinors $\Psi_{L/R}$. This term is not invariant under $SU(2)_L \times U(1)_Y$ gauge transformations, but adding a Yukawa term

$$\mathcal{L}_{\text{Yukawa}} = -y \bar{L}_L \Phi e_R + h.c., \quad (1.10)$$

coupling the fermion fields to the Higgs field, recovers the invariance and gives the fermions their masses. Here, y is the Yukawa coupling constant and \bar{L}_L is the $SU(2)_L$ doublet. With the vev, this results in the mass term for the charged leptons and down-type quarks of $-m_e(\bar{e}_L e_R + \bar{e}_R e_L)$ with $m_e = \frac{yv}{\sqrt{2}}$. With $\tilde{\Phi} = i\sigma_2 \Phi^*$, a similar Yukawa term can be written as $-y \bar{L}_L \tilde{\Phi} u_R + h.c.$, which leads to the masses of the up-type quarks.

1.1.4 Weak Interactions after Symmetry-Breaking

Stuff from my MSc thesis to re-write:

In the SM, weak interactions are mediated by the three massive bosons W^+ , W^- , and Z^0 [12]. The large boson masses ($m_W \sim 80 \text{ GeV}$, $m_Z \sim 90 \text{ GeV}$) result in a short range of the force of about $10 \times 10^{-18} \text{ m}$. Weak interactions carried by W^\pm bosons are called CC interactions, because charge is transferred between the interacting particles. In CC interactions, a neutrino is converted into its corresponding charged lepton or vice versa. Neutral current (NC) interactions are those mediated by Z^0 bosons. Here no charge is transferred. The Feynman diagrams for CC and NC interactions are shown in Figure 1.1.

The observed phenomenon of neutrino oscillations (see Section 1.3.3) is based on the fact that there is a mass difference between the three neutrino mass eigenstates.

Introduce SM EW NC/CC Lagrangian to build upon in the next chapter

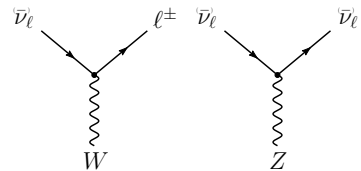


Figure 1.1: Feynman diagrams of charged-current (left) and neutral-current (right) neutrino weak interactions, taken from [11].

Plot is missing + for W and 0 for Z boson.

[12]: Thomson (2013), *Modern particle physics*

1.2 Beyond the Standard Model

Open questions related to neutrinos:

- ▶ question of neutrino nature, e.g. dirac or majorana?
- ▶ absolute mass values? (mass ordering + absolute mass scale)
- ▶ is there leptonic cp violation and what is the precise delta_cp value?
- ▶ what are the mixing angle values and is there a flavor principle
- ▶ is there additional effects like steriles, non-standard, lorentz violation

Are the fundamentals of the SM described above enough to explain *all* observed phenomena? Gravity cannot be explained by the SM, as it is incompatible with general relativity. Neither can the SM explain some cosmological observations like dark matter, and the matter-antimatter asymmetry, and it does not predict neutrinos to have mass, which is experimentally proven by neutrino oscillations, so some extensions to the SM is needed in order to explain them.

Cite and/or sidenote this.

Standard cosmology (Λ CDM) assumes that equal amounts of matter and anti-matter were produced in the early universe. However, the universe today is dominantly made up of matter. This so-called *baryon asymmetry* can be measured by the difference between the number densities of baryons and anti-baryons normalized to the number density of photons as

$$\eta_B = \frac{n_B - n_{\bar{B}}}{n_\gamma}, \quad (1.11)$$

cite this

where n_B , $n_{\bar{B}}$, and n_γ are the number densities of baryons, anti-baryons, and photons, respectively. Baryons are the dominant component with η_B being observed to be around 6×10^{-10} . Leptogenesis and EW baryogenesis are scenarios that could explain this phenomenon, where the former could be realized by the existence of heavy RH neutrinos.

- [13]: Davis et al. (1968), "Search for Neutrinos from the Sun"
- [14]: Fukuda et al. (1998), "Evidence for Oscillation of Atmospheric Neutrinos"
- [15]: Ahmad et al. (2002), "Direct Evidence for Neutrino Flavor Transformation from Neutral-Current Interactions in the Sudbury Neutrino Observatory"

cite neutrino oscillations/flavor conversions

The observation of neutrino flavor conversions and neutrino oscillations in a multitude of experiments[13–15] is the strongest evidence for physics beyond the SM measured in laboratories. The observation that neutrinos change their flavor while they propagate through space can only be explained, if at least two neutrinos have a non-zero mass. From the measurements and cosmological observations, we know that the masses are very small as compared to the lepton masses. Neither their existence, nor their smallness is not predicted by the SM, but adding additional RH neutrinos states to the theory could explain the origin of the observed non-zero neutrino masses and could be tested for by searching for corresponding signatures in experiments. But the addition of RH neutrino fields is not the only possible explanation for neutrino masses. Radiative neutrino mass mechanisms could also explain their origin and their smallness, but those would need the introduction of additional symmetries to the theory.

- [16]: Tanabashi et al. (2018), "Review of Particle Physics"
- [17]: Aker et al. (2022), "Direct neutrino-mass measurement with sub-electronvolt sensitivity"
- [18]: Alam et al. (2021), "Completed SDSS-IV extended Baryon Oscillation Spectroscopic Survey: Cosmological implications from two decades of spectroscopic surveys at the Apache Point Observatory"
- [19]: Aghanim et al. (2020), "Planck2018 results: VI. Cosmological parameters"

namedrop RH=sterile=HNL and why they are called like this based on the SM EW Lagrangian introduced above

Maybe also add this somehow: "From neutrino oscillation measurements the absolute mass scale cannot be determined, since they only depend on the mass differences, but there are upper limits on the sum of all neutrino masses from cosmological observations. These upper limits are typically between 0.3 and 1.3 eV [16]." "Actually 0.8 eV [17] from KATRIN and 1.2 eV [18, 19] from cosmological observations."

1.2.1 Mass Mechanisms

There are no RH neutrinos in the SM and therefore the mass mechanism described in Section 1.1.3, which couples the Higgs field to LH and RH Weyl fields, predicts them to be massless. From experimental observations it is known that at least two of the three neutrino generations need to have a non-zero mass. Assuming the existence of RH neutrinos fields ν_R , one way of producing the neutrino masses is by adding a Yukawa

coupling term similar to the one for up-type quarks mentioned in Section 1.1.3, to write the full Yukawa Lagrangian as

$$\mathcal{L}_{\text{Yukawa}} = -Y_{ij}^e \bar{L}_L^i \Phi e_R^j - Y_{ij}^\nu \bar{L}_L^i \tilde{\Phi} \nu_R^j + h.c. , \quad (1.12)$$

with i, j running over the three generations of leptons e, μ , and τ , and Y^e and Y^ν being the Yukawa coupling matrices. Diagonalizing the Yukawa coupling matrices through unitary transformations U^e and U^ν leads to the **Dirac mass term** in the mass basis as

$$\mathcal{L}_{\text{Dirac}}^{\text{mass}} = \frac{v}{\sqrt{2}} (\bar{e}_L M_e e_R - \bar{\nu}_L M_\nu \nu_R) , \quad (1.13)$$

where M_e and M_ν are the diagonal mass matrices of leptons and neutrinos, respectively. A purely Dirac mass term would not explain the smallness of the neutrino masses in a straightforward way. Only fine-tuning the Yukawa coupling constants to small values would lead to small neutrino masses.

An additional way of generating neutrino masses is by adding a Majorana mass term of the form

$$\mathcal{L}_{\text{Majorana}} = -\frac{1}{2} M_{ij} (\nu_R^i)^c \nu_R^j + h.c. , \quad (1.14)$$

with M_{ij} being the Majorana mass matrix and the indices i, j running over all N_R RH neutrino generations. The superscript c denotes the charge conjugate field. Combining the charge conjugated RH neutrino fields with the LH neutrino fields as

$$N = \begin{pmatrix} \nu_L \\ \nu_R^c \end{pmatrix} , \quad (1.15)$$

with ν_R containing the N_R RH fields. The full neutrino mass Lagrangian is then given by the combined **Dirac and Majorana mass term** as

$$\mathcal{L}_{\text{Dirac+Majorana}}^{\text{mass}, \nu} = \frac{1}{2} N^T \hat{C} M^{D+M} N + h.c. , \quad (1.16)$$

and the mass matrix is given by

$$M^{D+M} = \begin{pmatrix} 0 & (M^D)^T \\ M^D & M^R \end{pmatrix} . \quad (1.17)$$

On top of explaining the origin of neutrino masses itself, a combined Dirac and Majorana mass term could also solve the question of their smallness. If the mass of the RH neutrinos is very large, the masses of the active neutrino flavors is suppressed, which is known as *see-saw mechanism*.

1.2.2 Observational Avenues for Right-Handed Neutrinos

- ▶ oscillations searches for light steriles
- ▶ potential searches for heavy steriles

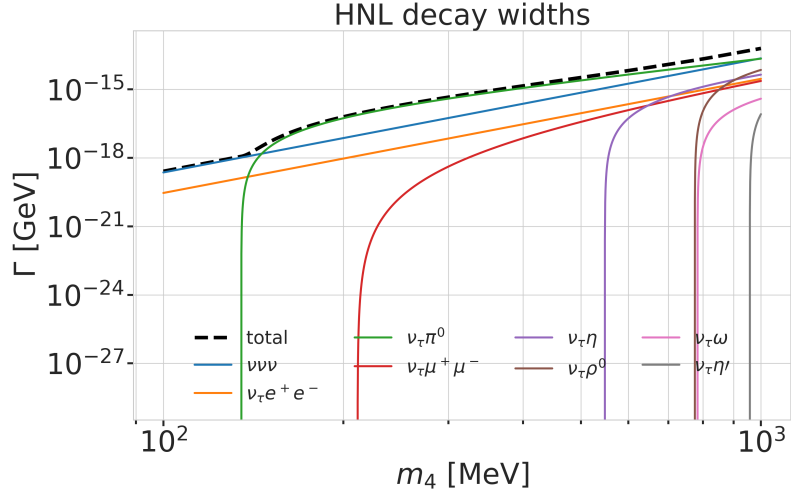


Figure 1.2: Decay widths of the HNL within the mass range considered, calculated based on the results from [20]. Given the existing constraints on $|U_{e4}|^2$ and $|U_{\mu 4}|^2$, we consider that the corresponding decay modes are negligible.

1.2.3 Searching for Heavy Neutral Leptons

Collider

Nuclear Decay

Extracted Beamlines

Atmospheric and Solar

Cosmological and Astrophysical

1.3 Atmospheric Neutrinos as Source of Heavy Neutral Leptons

write some interlude to motivate atm. neutrinos as source for HNL searches/production etc.

[16]: Tanabashi et al. (2018), “Review of Particle Physics”

1.3.1 Production of Neutrinos in the Atmosphere

The analysis performed in this work is based on the sample of neutrinos observed in IceCube DeepCore at energies below 100 GeV. At these energies, the flux exclusively originates in the Earth’s atmosphere. Highly relativistic cosmic rays (protons and heavier nuclei [16]) interact in the upper atmosphere, producing showers of secondary particles. Neutrinos are produced in decays of charged pions and kaons (π and K mesons) present in those showers, where the dominant contribution comes from the decay chain

$$\begin{aligned} \pi^\pm &\rightarrow \mu^\pm + \nu_\mu (\bar{\nu}_\mu) , \\ \mu^\pm &\rightarrow e^\pm + \bar{\nu}_\mu (\nu_\mu) + \nu_e (\bar{\nu}_e) , \end{aligned} \quad (1.18)$$

where muon neutrinos ν_μ and muons μ^\pm are produced in the first decay and both electron and muon neutrinos $\nu_{e/\mu}$ are produced in the second decay. Atmospheric muons, which are also produced in these decays, are the main background component for IceCube DeepCore analyses.

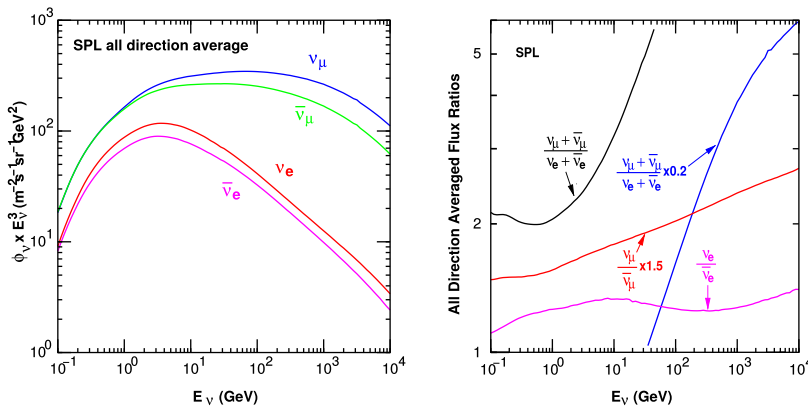


Figure 1.3: The atmospheric fluxes of different neutrino flavors as a function of energy (left) and the ratios between muon neutrinos and electron neutrinos as well as the ratios between neutrinos and antineutrinos for both those flavors (right). Results from the calculations performed for the geographic South Pole, taken from [21].

The different atmospheric flux components are shown in Figure 1.3 (left), for a much broader energy range than relevant for this work. Both neutrinos and antineutrino fluxes are shown for electron and muon neutrinos and all fluxes are the directionally averaged expectation calculated at the South Pole. Muon neutrinos are dominating the flux and from Equation 1.18 the naive assumption would be that the ratio between muon and electron neutrinos is $(\nu_\mu + \bar{\nu}_\mu)/(\nu_e + \bar{\nu}_e) = 2$. This is roughly true at energies below 1 GeV, where all muons decay in flight, but at larger energies muons can reach the detector before decaying, which increases the ratio to approximately 10:1 at around 100 GeV. Additionally, kaon decays start to contribute which also increases the number of muons and muon neutrinos. The increasing ratio can be seen in Figure 1.3 (right), which also shows the ratio between neutrinos and antineutrinos for both flavors.

Charged mesons or tau particles can also be produced in cosmic ray interactions. Their decays lead to the production of tau neutrinos. At the energies relevant for this work however, the resulting tau neutrino flux is negligible as compared to the muon neutrino flux [22] and is not considered in the analysis. This is because both charged mesons and tau particles are much heavier than pions and kaons and therefore their production is suppressed at high energies.

[22]: Fedynitch et al. (2015), “Calculation of conventional and prompt lepton fluxes at very high energy”

1.3.2 Interactions with Nuclei

Say something about atmospheric neutrino flux uncertainties, based on recent JP/Anatoli papers.

The neutrino detection principle of IceCube DeepCore is explained in Chapter ?? and relies on the weak interaction processes between neutrinos and the nuclei of the Antarctic glacial ice. At neutrino energies above 5 GeV, the cross-sections are dominated by *deep inelastic scattering (DIS)*, where the neutrino is energetic enough to resolve the underlying structure of the nucleons and interact with one of the composing quarks individually. As a result the nucleon breaks and a shower of hadronic secondary particles is produced. Depending on the type of interaction, the neutrino either remains in the final state for NC interactions or is converted into its charged lepton counterpart for CC interactions. The CC DIS interactions have the form

$$\begin{aligned} \nu_l + N &\rightarrow l^- + X , \\ \bar{\nu}_l + N &\rightarrow l^+ + X , \end{aligned} \quad (1.19)$$

where $\nu_l/\bar{\nu}_l$ and l^-/l^+ are the neutrino/antineutrino and its corresponding lepton/antilepton, and l can be either an electron, muon, or tau. N is the nucleon and X stands for any set of final state hadrons. The NC DIS interactions are

$$\begin{aligned} \nu_l + N &\rightarrow \nu_l + X \text{ and} \\ \bar{\nu}_l + N &\rightarrow \bar{\nu}_l + X . \end{aligned} \quad (1.20)$$

Figure 1.4 shows the Feynman diagrams for both processes DIS interac-

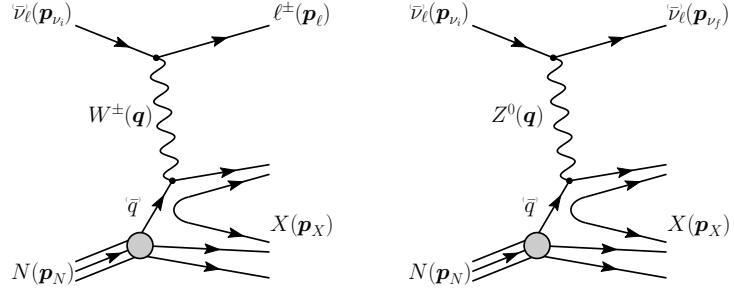


Figure 1.4: Feynman diagrams for deep inelastic scattering of a neutrino with a nucleon via charged-current (left) and neutral current (right) interactions. p_{ν_i} , p_N and p_{ν_f} , p_l , p_X are the input and output four-momenta, while q is the momentum transfer. Taken from [11].

tions have a roughly linear energy dependent cross-section above ~ 20 GeV and are well measured and easy to theoretically calculate. They are the primary interaction channel for neutrinos detected with IceCube.

At energies below 5 GeV, *quasi-elastic scattering (QE)* and *resonant scattering (RES)* become important. At these energies the neutrinos interact with the approximately point-like nucleons, without breaking them up in the process. RES describes the process of a neutrino scattering off a nucleon producing an excited state of the nucleon in addition to a charged lepton. It is the dominant process at 1.5 GeV to 5 GeV for neutrinos and 1.5 GeV to 8 GeV for antineutrinos. Below 1.5 GeV QE is the main process, where protons are converted to neutrons in antineutrino interactions and vice-versa for neutrino interactions. Additionally, a charged lepton corresponding to the neutrino/antineutrino flavor is produced. The cross-sections of QE and RES scattering processes are not linear in energy and the transition region from QE/RES to DIS is poorly understood. The total cross-sections and their composition is shown in Figure 1.5. It can be seen that the interaction cross-sections are very small at the order of 10^{-38} cm 2 . This is the reason why very large volume detectors are required to measure atmospheric neutrinos with sufficient statistics to perform precision measurements of their properties. The interaction length of a neutrino with $E_\nu = 10$ GeV is of $\mathcal{O}(10 \times 10^{10}$ km), for example.

1.3.3 Oscillations

So far we have described neutrinos in their flavor eigenstates, which are relevant for weak interactions. In the SM three-neutrino model the weak flavor states are ν_e , ν_μ , and ν_τ , which relate them to the charged leptons they interact with in CC interactions. There is a second way of describing neutrino wave functions based on their Hamiltonian eigenvalues [24], namely as the mass eigenstates ν_1 , ν_2 , and ν_3 . These states are related to the flavor eigenstates by the unitary, 3x3 Pontecorvo-Maki-Nakagawa-Sakata

[24]: Bilenky et al. (1978), "Lepton mixing and neutrino oscillations"

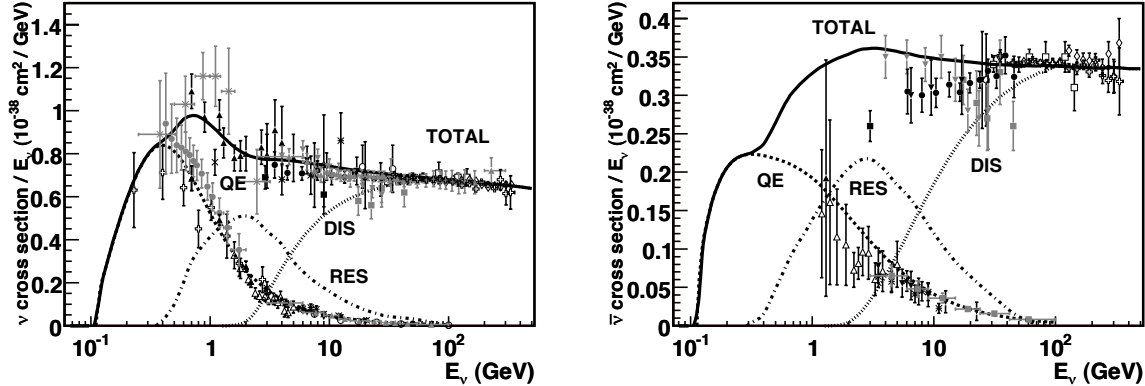


Figure 1.5: Total neutrino (left) and antineutrino (right) per nucleon cross-section divided by neutrino energy plotted against energy. The three main scattering processes quasi-elastic scattering (QE), resonant scattering (RES), and deep-inelastic scattering (DIS) are shown. Taken from [23].

(PMNS) matrix U , where the flavor states are a superposition of the mass states as

$$|\nu_\alpha\rangle = \sum_k U_{\alpha k}^* |\nu_k\rangle , \quad (1.21)$$

with the weak flavor states $|\nu_\alpha\rangle$, $\alpha = e, \mu, \tau$, and the mass states $|\nu_k\rangle$ with $k = 1, 2, 3$. The mixing matrix can be parameterized as [16]

$$U = \begin{pmatrix} 1 & 0 & 0 \\ 0 & c_{23} & s_{23} \\ 0 & -s_{23} & c_{23} \end{pmatrix} \begin{pmatrix} c_{13} & 0 & s_{13}e^{-i\delta_{CP}} \\ 0 & 1 & 0 \\ -s_{13}e^{i\delta_{CP}} & 0 & c_{13} \end{pmatrix} \begin{pmatrix} c_{12} & s_{12} & 0 \\ -s_{12} & c_{12} & 0 \\ 0 & 0 & 1 \end{pmatrix}, \quad (1.22)$$

where $c_{ij} = \cos \theta_{ij}$ and $s_{ij} = \sin \theta_{ij}$ are cosine and sine of the mixing angle θ_{ij} , that defines the strength of the mixing between the mass eigenstates i and j , and δ_{CP} is the neutrino CP-violating phase.

[16]: Tanabashi et al. (2018), "Review of Particle Physics"

Describing neutrinos in their mass state is crucial to understand their propagation through space and time. Their propagation in vacuum can be expressed by applying a plane wave approach, where the mass eigenstates evolve as

$$|\nu_k(t)\rangle = e^{-iE_k t/\hbar} |\nu_k\rangle . \quad (1.23)$$

add current BF values from nufit or so?

The energy of the mass eigenstate $|\nu_k\rangle$ is $E_k = \sqrt{\vec{p}^2 c^2 + m_k^2 c^4}$, with momentum \vec{p} and mass m_k , \hbar is the reduced Planck constant, and c is the speed of light in vacuum. The existence of non-zero, non-equal masses and the neutrino mixing relation in Equation 1.21, lead to the observed phenomenon of neutrino oscillations. Oscillations mean that a neutrino changes from its initial flavor, that it was produced with, to another flavor and back after traveling a certain distance. A neutrino is produced as a flavor eigenstate $|\nu_\alpha\rangle$ in a CC weak interaction, but its propagation happens as the individual mass states it is composed of. The probability of finding the neutrino with initial flavor $|\nu_\alpha\rangle$ in the flavor state $|\nu_\beta\rangle$ after the time t is calculated as

$$P_{\nu_\alpha \rightarrow \nu_\beta}(t) = |\langle \nu_\beta | \nu_\alpha(t) | \nu_\beta | \nu_\alpha(t) \rangle|^2 , \quad (1.24)$$

by applying Fermi's Golden Rule [25], which defines the transition rate from one eigenstate to another by the strength of the coupling between

[25]: Dirac (1927), "The Quantum Theory of the Emission and Absorption of Radiation"

them. This coupling strength is the square of the matrix element and using the fact that the mixing matrix is unitary ($U^{-1} = U^\dagger$) to describe the mass eigenstates as flavor eigenstates, we find the time evolution of the flavor state $|\nu_\alpha(t)\rangle$, which can be inserted into Equation 1.24 to find the probability as

$$P_{\nu_\alpha \rightarrow \nu_\beta}(t) = \sum_{j,k} U_{\beta j}^* U_{\alpha j} U_{\beta k} U_{\alpha k}^* e^{-i(E_k - E_j)t/\hbar}. \quad (1.25)$$

The indices j and k run over the mass eigenstates. We can approximate the energy as

$$E_k \approx E + \frac{c^4 m_k^2}{2E} \quad \longrightarrow \quad E_k - E_j \approx \frac{c^4 \Delta m_{kj}^2}{2E}, \quad (1.26)$$

for small neutrino masses compared to their kinetic energy. Here, $\Delta m_{kj}^2 = m_k^2 - m_j^2$ is the mass-squared splitting between states k and j . Replacing the time in Equation 1.25 by the distance traveled by relativistic neutrinos $t \approx L/c$ we get

$$\begin{aligned} P_{\nu_\alpha \rightarrow \nu_\beta}(t) &= \delta_{\alpha\beta} - 4 \sum_{j>k} \text{Re}(U_{\beta j}^* U_{\alpha j} U_{\beta k} U_{\alpha k}^*) \sin^2\left(\frac{c^3 \Delta m_{kj}^2}{4E\hbar} L\right) \\ &\quad + 2 \sum_{j>k} \text{Im}(U_{\beta j}^* U_{\alpha j} U_{\beta k} U_{\alpha k}^*) \sin\left(\frac{c^3 \Delta m_{kj}^2}{4E\hbar} L\right), \end{aligned} \quad (1.27)$$

which is called the survival probability if $\alpha = \beta$, and the transition probability if $\alpha \neq \beta$. Once again, this probability is only non-zero if there are neutrino mass eigenstates with masses greater than zero. Additionally, there must be a mass-squared difference Δm^2 and non-zero mixing between the states. Since we assumed propagation in vacuum in Equation 1.23, the transition and survival probabilities correspond to vacuum mixing.

say something about how this changes with matter

1.3.4 Testing Heavy Neutral Leptons with Atmospheric Neutrinos

Re-write/re-formulate this section (copied from HNL technote).

[26]: Yanagida (1980), "Horizontal Symmetry and Masses of Neutrinos"

Produce similar styled plot for these limits

[32]: Coloma et al. (2017), "Double-Cascade Events from New Physics in Icecube"

The Minimal Standard Model Extension

Extensions to the Standard Model (SM) that add *Heavy Neutral Leptons* (HNLs) provide a good explanation for the origin of neutrino masses through different seesaw mechanisms [26]. While the mixing with ν_e/μ is strongly constrained ($|U_{\alpha 4}^2| \lesssim 10^{-5} - 10^{-8}$, $\alpha = e, \mu$), the mixing with ν_τ is much harder to probe due to the difficulty of producing and detecting ν_τ . Figure 1.6 shows the current limits on the τ -sterile mixing space for HNL masses between 0.1 GeV-10 GeV. As was first pointed out in [32], the atmospheric neutrino flux observed in IceCube offers a way to constrain the neutrino-HNL mixing parameters. By using the large fraction of atmospheric ν_μ events that oscillate into ν_τ before they reach the detector, the less constrained τ -sterile mixing space can be explored. In this document, we present the methodology and strategy of a search for HNLs with IceCube DeepCore. These additional RH neutrinos can

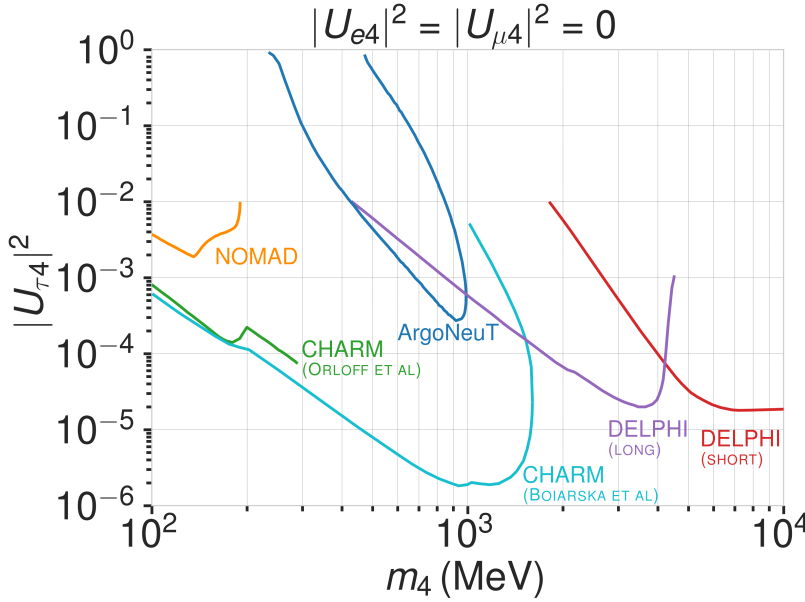


Figure 1.6: Current $|U_{\tau 4}^2| - m_4$ limits from NOMAD [27], ArgoNeut [28], CHARM [29, 30], and DELPHI [31].

be included in the Standard Model (SM) by extending the PMNS matrix to at least a 3x4 matrix as

$$\begin{pmatrix} \nu_e \\ \nu_\mu \\ \nu_\tau \\ \nu_s \end{pmatrix} = \begin{pmatrix} U_{e1} & U_{e2} & U_{e3} & U_{e4} \\ U_{\mu 1} & U_{\mu 2} & U_{\mu 3} & U_{\mu 4} \\ U_{\tau 1} & U_{\tau 2} & U_{\tau 3} & U_{\tau 4} \\ U_{s1} & U_{s2} & U_{s3} & U_{s4} \end{pmatrix} \begin{pmatrix} \nu_1 \\ \nu_2 \\ \nu_3 \\ \nu_4 \end{pmatrix}, \quad (1.28)$$

where the components with index 4 define the mixing between the flavor states and the fourth sterile mass state, respectively. Note here that this is not a theoretically fully consistent picture, but rather the phenomenologically minimal model to be tested by this analysis. This can hopefully be put into the larger context of several fully consistent models, later. Due to the singlet nature of the RH neutrinos, they only interact weakly, inheriting these interactions from their LH neutrino counterparts via mixing. This mixing of the HNLs with the electron, muon, and tau neutrinos can be probed and constrained as a function of the HNL mass by searching for their production and decay. In [32, 33] this search is mainly motivated through two experimental arguments. Secondly, IceCube is ideally placed to explore the yet unconstrained $|U_{\tau 4}|^2 - m_4$ phase-space that is not easily accessible by accelerator-based experiments.

In order to probe the τ -sterile mixing parameter, it is required to look at interactions involving τ neutrinos. However, most neutrinos produced in cosmic ray interactions with the atmosphere are ν_e or ν_μ . Therefore, we need these neutrinos to oscillate to the τ flavor before reaching the detector. For this to happen at the considered energies a traveled distance of the order of the earth diameter is necessary. This is why our signal is mostly up-going and passing through the whole earth.

To explain the signature we can observe in IceCube we first have to revisit the weak interactions that the HNL inherits from its LH counterpart through mixing. We will be following the derivation in [20]. Extending the SM by n additional RH neutrinos, ν_i ($i = 3 + n$), leads to the mass

[32]: Coloma et al. (2017), "Double-Cascade Events from New Physics in Icecube"

[33]: Coloma (2019), "Icecube/DeepCore tests for novel explanations of the Mini-BooNE anomaly"

This section really needs to be re-written to motivate the search for HNLs from a more generic point of view (e.g. to explain neutrino masses)

This section definitely needs to be elaborated in a little more detail

[20]: Coloma et al. (2021), "GeV-scale neutrinos: interactions with mesons and DUNE sensitivity"

Lagrangian

$$\mathcal{L}_v^{\text{mass}} \supset - \sum_{\alpha=e,\mu,\tau} \sum_{i=4}^{3+n} Y_{\nu,\alpha i} \bar{L}_{L,\alpha} \tilde{\phi} \nu_i - \frac{1}{2} \sum_{i=4}^{3+n} M_i \bar{\nu}_i \nu_i^c + h.c., \quad (1.29)$$

in a basis where the Majorana mass terms are diagonal. $Y_{\nu,\alpha i}$ are the Yukawa couplings to the lepton doublets and M the Majorana masses for the heavy singlets. $L_{L,\alpha}$ stands for the SM LH lepton doublet of flavor α while ϕ is the Higgs field, and $\tilde{\phi} = i\sigma_2\phi^*$ and $\nu_i^c \equiv C\bar{\nu}_i^t$, with $C = i\gamma_0\gamma_2$ in the Weyl representation. The full neutrino mass matrix with the Higgs vacuum expectation value $v/\sqrt{2}$ reads

Not adding information about the case where the neutrinos have Dirac or pseudo-Dirac masses

$$\mathcal{M} = \begin{pmatrix} 0_{3 \times 3} & Y_\nu v / \sqrt{2} \\ Y_\nu^t v / \sqrt{2} & M \end{pmatrix}, \quad (1.30)$$

and can be diagonalized by a $(3+n) \times (3+n)$ full unitary rotation U , that itself leads to neutrino masses upon diagonalization, additionally manifesting the mixing between active neutrinos and heavy states. The resulting model consists of 3 light SM neutrino mass eigenstates ν_i ($i = 1, 2, 3$) and n heavier states, as introduced above. The flavor states will now consist of a combination of light and heavy states

$$\nu_\alpha = \sum_{i=1}^{3+n} U_{\alpha i} \nu_i, \quad (1.31)$$

and the leptonic part of the EW Lagrangian can be written as

$$\begin{aligned} \mathcal{L}_{\text{EW}}^\ell = & \frac{g}{\sqrt{2}} W_\mu^+ \sum_\alpha \sum_i U_{\alpha i}^* \bar{\nu}_i \gamma^\mu P_L \ell_\alpha + \frac{g}{4c_w} Z_\mu \\ & \times \left\{ \sum_{i,j} C_{ij} \bar{\nu}_i \gamma^\mu P_L \nu_j + \sum_\alpha \bar{\ell}_\alpha \gamma^\mu [2s_w^2 P_R - (1-2s_w^2) P_L] \ell_\alpha \right\} + h.c., \end{aligned}$$

where $c_w \equiv \cos \theta_w$, $s_w \equiv \sin \theta_w$, and θ_w the SM weak mixing angle. P_L and P_R are the left and right projectors, respectively, while

$$C_{ij} \equiv \sum_\alpha U_{\alpha i}^* U_{\alpha j}. \quad (1.32)$$

The indices now sum over all $(3+n)$ flavor and mass states.

Based on this formulation and assuming that only the mixing with the tau sector is open ($|U_{\alpha 4}^2| = 0$, $\alpha = e, \mu$), the relevant production diagram of the HNL can be drawn as shown in Figure 1.7. Alongside the fourth heavy mass state, a Hadronic cascade is produced. The heavy mass state will travel for some distance (dependent on mass and mixing) before it decays. The subsequent decay processes are depicted in Figure 1.8. It can be a CC or NC decay and both leptonic and mesonic modes are possible (dependent on the mass). This will produce a tau or a tau neutrino and another cascade that can be EM or Hadronic. The branching ratios corresponding to the decay modes of the HNL for the mass range of interest (i.e. between 100 MeV and 1 GeV) are shown in Figure 1.9a as a function of the HNL mass.

Production and Decay in IceCube DeepCore

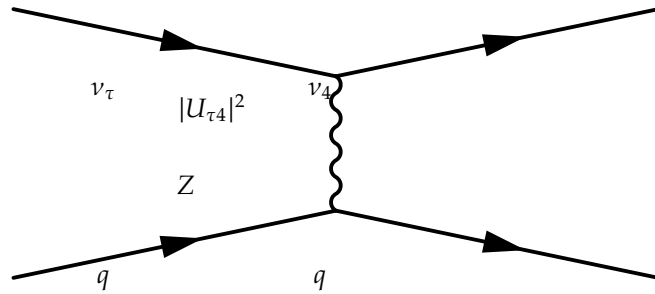


Figure 1.7: Production of a sterile neutrino in the up-scattering of a tau neutrino.

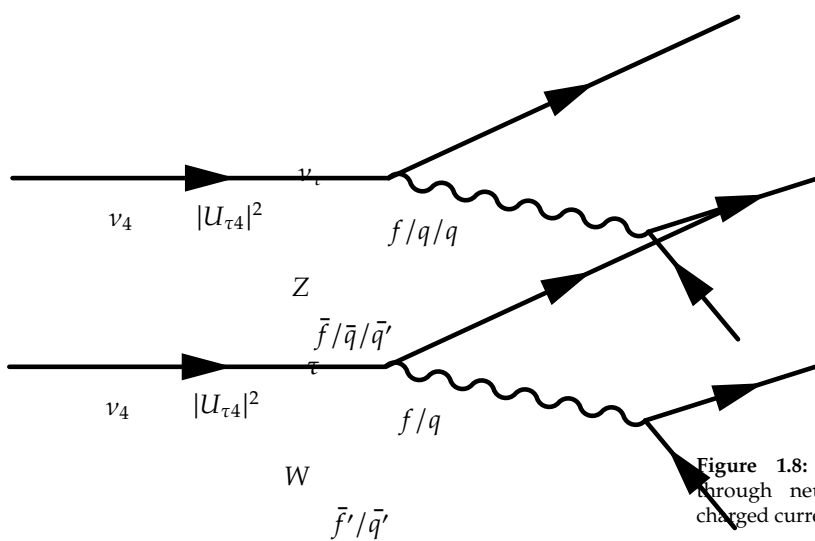


Figure 1.8: Sterile neutrino decay through neutral current (left) and charged current (right).

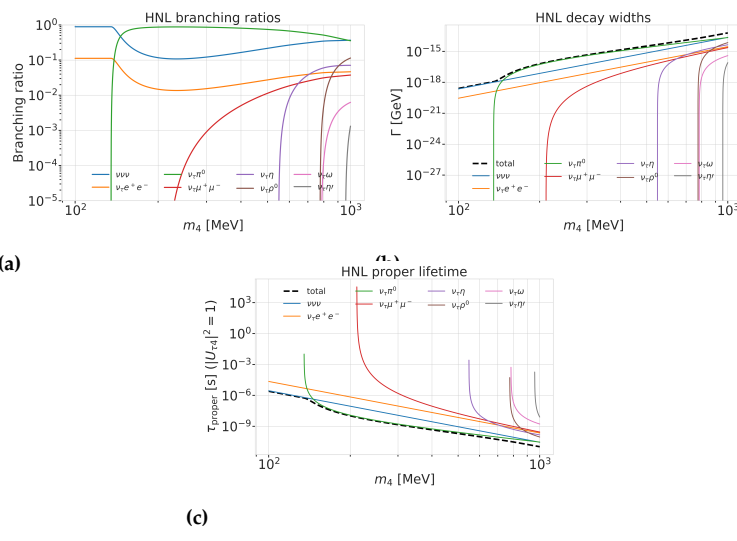


Figure 1.9: Branching ratios, decay widths, and proper lifetime of the HNL within the mass range considered, calculated based on the results from [20].

Detecting Low Energetic Double Cascades

2

2.1 Reconstruction

2.1.1 Table-Based Minimum Likelihood Algorithms

2.1	Reconstruction	15
2.2	Cross Checks	15
2.3	Performance	16

2.1.2 Double Cascade Hypothesis

2.1.3 Modification to Low Energy Events

2.2 Cross Checks

2.2.1 Simplistic Sets

After generation the events are processed with standard Photon, Detector, L1, and L2 processing and then Taupede+MuMillipede is run on top of the L2 files. Multiple versions with different parameters were produced, some with the OscNext baseline parameters, some without detector noise (in Det level) and some with h2-50cm holeice model, to match the holeice model that was used to generate the photonics tables.

BrightDom Cleaning To investigate the effect of the BrightDom cleaning cut the 194601 set without detector noise (and baseline hole ice model) is used. The BrightDom cleaning is needed to stop a few DOMs with many photon hits to drive the reconstruction because this leads to large biases in the energy estimations. Historically, the BrightDom cleaning was removing all DOMs that had a charge larger than 10 times the mean charge. After quickly checking some charge distributions and how the mean behaves it was clear that the cut should better be defined based on a metric that is less affected by outliers, like the median. Figure ?? shows where the mean and the median are located for an example event. The cut was re-defined to use the median instead of the mean and 10% of the simulation were processed with [Taupede](#) using 30x and 100x the median as BrightDom cutoff. Figure ?? shows where these values fall for the same example event.

As a quick check of the performance of both cuts the decay length resolution/bias and the resolutions/biases of all energies were checked. The reconstructed decay length is almost not affected by applying this cut, which is as expected, because it is mostly dependent on the arrival time of the photons. The effect on the reconstructed energy is much stronger, where a looser cut (100x) shows a significantly larger bias than the tighter cut at (30x). Even though this was not a highly sophisticated optimization of the BrightDom cut, an improvement was achieved by changing from mean to median and selecting the tighter cut (of the two tested). It's hard to tell how this would perform for high energy events, but I'm quite certain that a definition based on the median would be more reliable than on the mean.

2.3 Performance

2.3.1 Energy/Decay Length Resolution

describe the "good fit" selection

2-D Histograms

Things to mention about the 2d-hists:

- ▶ total energy resolution looks very good, above 10 GeV it's almost unbiased and the 1-sigma resolution band is below 20 %
- ▶ individual cascade resolutions mirror this behavior, but are starting to stabilize in energy at lower energies around 5 GeV to 6 GeV with a broader resolution band of 50 %, but reducing drastically with increasing energy (down to 20% at 100 GeV)
- ▶ interestingly, the second cascade energy reconstruction performs slightly worse, although they have the same energy ranges. This could hint at an asymmetry in the reconstruction process (might relate to how the two cascades are parameterized) or be due to the different positions and the dominantly up-going direction used in the sampling combined with the DOMs looking down (relate this to the sampling distributions explained/shown in the previous chapter)
- ▶ the decay length resolution looks much worse. In the region between 20 m and 80 m it's roughly unbiased, but 1-sigma resolution band is quite wide with a lot of outliers towards short reconstructed lengths. Below 20 m the reconstructed lengths are always over-estimating the true and above 80 m a population of events start to dominate where the decay lengths isn't getting reconstructed at all, which might indicate that one of the cascades wasn't observers. (Relate to the fact that this marginalizes over all energies, meaning also all events which have one cascade with very low energy are included here.)
- ▶ another interesting feature is the band of reconstructed lengths around 100 m, which is probably related to the spacing between most of the strings, which favors the reconstruction to be around this value, because that's the distance at which light can be observed, just from the fact that the DOMs are spaced at this distance (for low energetic cascades, this can dominate the reconstruction)

Energy Resolution

Things to mention about the energy resolution:

- ▶ Here it can be seen more clearly how the median total energy resolution starts to stabilize around 0.0 at 10 GeV, while for lower energies the reconstruction is over-estimating the true energy. This is a known behavior of energy reconstructions in IceCube, which is mainly due to a selection effect. Only events with a certain amount of light can be reconstructed, which means that the ones with true small energies that are still in the sample are events with over average light production due to fluctuations or other effects?

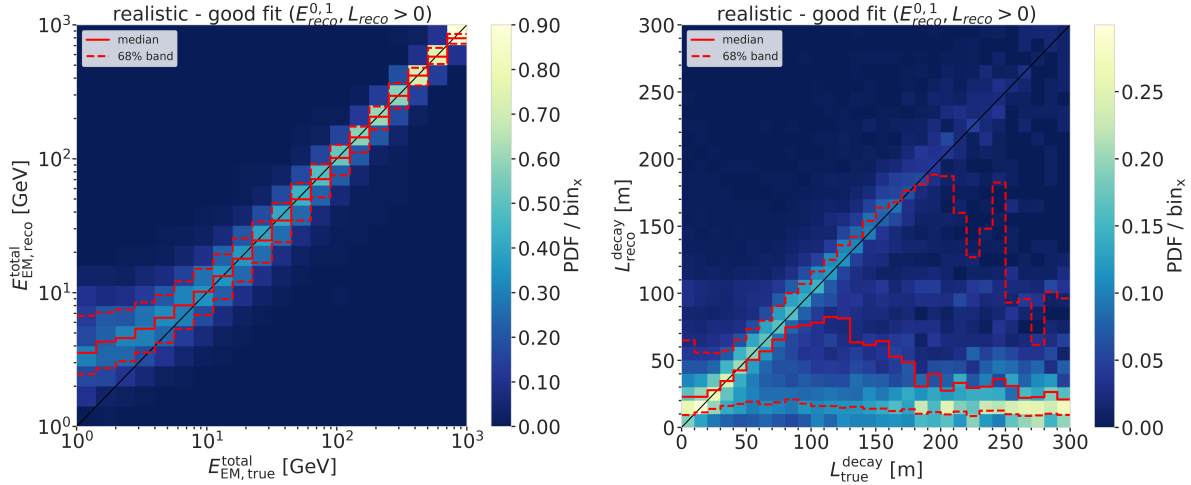


Figure 2.1

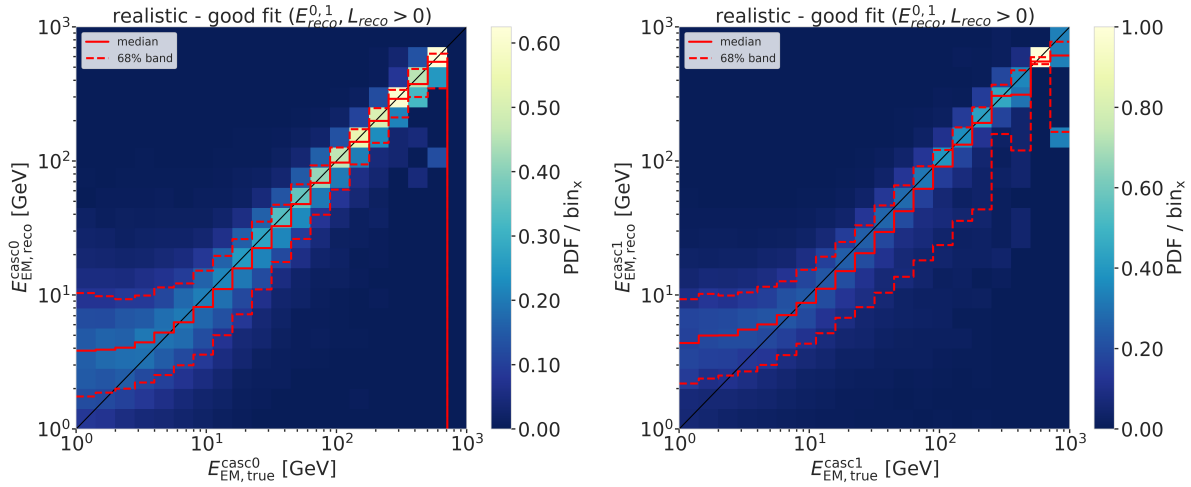


Figure 2.2

Decay Length Resolution

Things to mention about the decay length resolution:

- ▶ As already mentioned before, the decay length resolution is much worse than the energy resolutions. Figure 2.4 also shows that the median is below 0.0 for short true length and above 0.0 and approaching 1.0 for long true lengths.
- ▶ To investigate whether this is really due to the fact that one of the cascades is not observed, the decay length resolution was plotted against the total energy of the event and the minimum energy of the two cascades Figure 2.5.
- ▶ It can be seen that the median of the decay length resolution stabilizes at 0.0 for a total energy above 20 GeV, but the spread of the distribution is still quite large with a 1-sigma band of 80 % to 100 %.
- ▶ From the plot against the minimum energy it can be seen that the decay length resolution starts to be unbiased for a minimum energy of the cascades of 7 GeV, with an equivalently large spread.

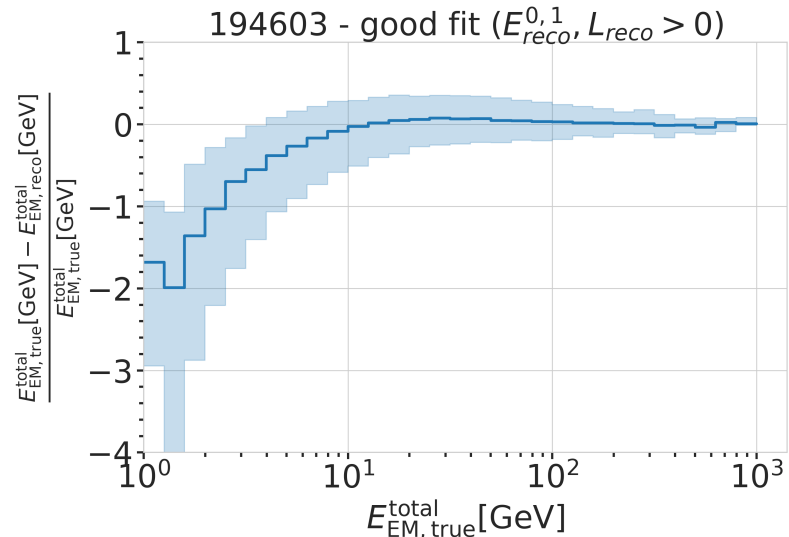


Figure 2.3

- ▶ A preliminary takeaway from this is that the decay length reconstruction is not reliable at all for events with a total energy below 20 GeV or a minimum cascade energy below 7 GeV.

2.3.2 Double Cascade Classification

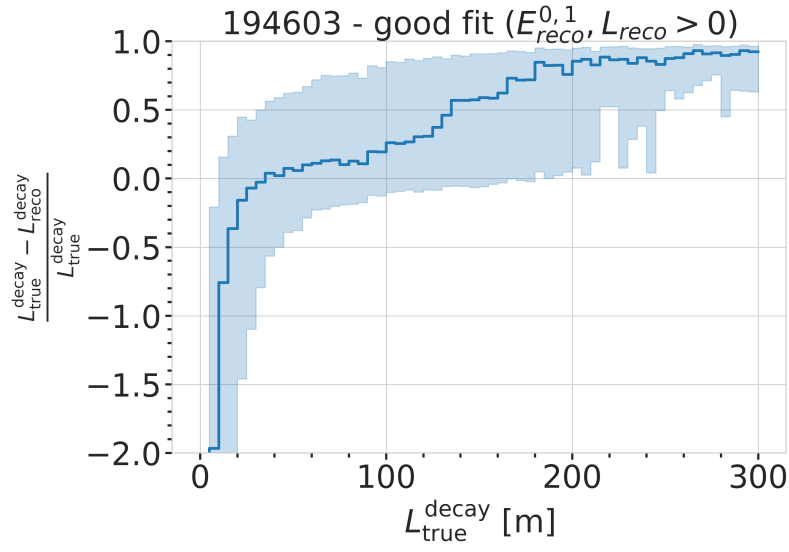


Figure 2.4

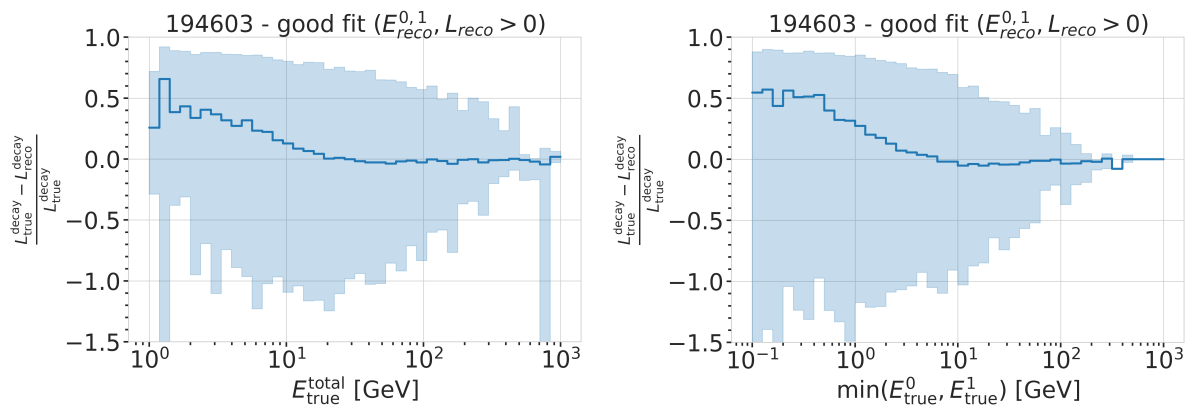


Figure 2.5

Search for an Excess of Heavy Neutral Lepton Events

3

The measurement performed in this thesis is the search for an excess of HNL events in the 10 years of IceCube DeepCore data. In principle the two physics parameters to be probed are the mass of the HNL, m_4 , and the mixing between the fourth heavy mass state and the SM τ sector, $|U_{\tau 4}|^2$. Since the mass itself influences the production and decay kinematics of the event and the accessible decay modes, individual mass sets were produced as described in Section ???. The mass slightly influences the energy distribution, while the mixing both changes the overall scale of the HNL events and the shape in energy and PID. IceCube DeepCore is suited to measure the excess which appears around and below 20 GeV, due to its production from the atmospheric tau neutrinos, although a reduced lower energy threshold could improve the analysis. The measurement will be performed for the three mass sets individually, while the mixing is the parameter that can be varied continuously and will be measured in the fit.

3.1 Final Level Sample

The final level sample of this analysis always consists of the neutrino and muon MC introduced in Section ?? and one of the three HNL samples explained in Section ???. All of those simulation sets and the 10 years of IceCube DeepCore data are processed through the full processing and event selection chain described in Section ?? leading to the final level sample. Since applying the last cuts from Section ?? leaves an insignificant amount of pure noise events in the sample, the noise simulation is not included in the analysis and won't be listed here.

3.1.1 Expected Rates/Events

The rates and the expected number of events for the SM background are shown in Table 3.1. The explicit detector livetime in the 10 years data taking period is 9.28 years. The rates are calculated by summing the weights of all events in the final level sample, while the uncertainties are calculated by taking the square root of the sum of the weights squared. The expected number of events is calculated by multiplying the rate with the livetime. The individual fractions show that this sample is neutrino dominated where the majority of events are ν_μ -CC events.

3.1	Final Level Sample	21
3.2	Statistical Analysis	23
3.3	Analysis Checks	23
3.4	Results	25

add information about the matter profile used

add information about the oscillation probability calculation and the software used for it

Should I adapt the total numbers to match the sum of the rounded individual parts?

Type	Rate [mHz]	Events (in 9.28 years)	Fraction [%]
ν_μ^{CC}	0.3531	103321 ± 113	58.9
ν_e^{CC}	0.1418	41490 ± 69	23.7
ν_{NC}	0.0666	19491 ± 47	11.1
ν_τ^{CC}	0.0345	10094 ± 22	5.8
μ	0.0032	936 ± 15	0.5
total	0.5991	175336 ± 143	100.0

Table 3.1: Final level rates and event expectation of the SM background particle types.

Table 3.2 shows the rates and expected number of events for the HNL signal simulation. The expectation depends on the mass and the mixing and shown here are two example mixings for all the three masses that are being tested in this work. A mixing of 0.0 would result in no HNL events at all. It can already be seen that for the smaller mixing of $|U_{\tau 4}|^2 = 10^{-3}$ the expected number of events is very low, while at the larger mixing of $|U_{\tau 4}|^2 = 10^{-1}$ the number is comparable to the amount of muons in the background sample.

Table 3.2: Final level rates and event expectations of the HNL signal for all three masses and two example mixing values.

HNL mass	Rate [μHz]	Events (in 9.28 years)
$ U_{\tau 4} ^2 = 10^{-1}$		
0.3 GeV	3.3298 ± 0.0053	974.5 ± 1.6
0.6 GeV	3.0583 ± 0.0058	895.0 ± 1.7
1.0 GeV	2.4988 ± 0.0059	731.3 ± 1.7
$ U_{\tau 4} ^2 = 10^{-3}$		
0.3 GeV	0.0057	1.67 ± 0.01
0.6 GeV	0.0220	6.44 ± 0.01
1.0 GeV	0.0248	7.27 ± 0.01

3.1.2 Analysis Binning

[34]: Yu et al. (2023), “Recent neutrino oscillation result with the IceCube experiment”

The identical binning to the analysis performed in [34] is used. It was chosen such that the track-like bin has the largest ν_μ -CC fraction. Extend the binning towards lower energies or increasing the number of bins did not improve the HNL sensitivities significantly. It also has to be considered that sufficient data events need to end up in the individual bins to result in a good fit, which was already investigated in the previous analysis. To mitigate the low data statistics, a few bins were not taken into account in the analysis. There are three bins in PID (cascade-like, mixed and track-like), 12 bins in reconstructed energy, and 8 bins in cosine of the reconstructed zenith angle as specified in Table 3.3. Originally, there were two more bins in $\cos(\theta)$, which were removed to reduce muons coming from the horizon and some low energy bins in the cascade-like bin are removed due to the low event statistics.

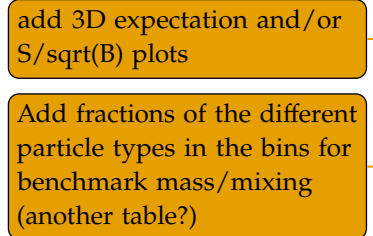


Table 3.3: Three dimensional binning used in the analysis. All variables are from the FLERCNN reconstruction explained in Section ??.

Variable	N_{bins}	Edges	Step
P_ν	3	[0.00, 0.25, 0.55, 1.00]	linear
E	12	[5.00, 100.00]	logarithmic
$\cos(\theta)$	8	[-1.00, 0.04]	linear

3.2 Statistical Analysis

3.2.1 Low Energy Analysis Framework

The analysis is performed using the PISA [35] [36] software framework, which was developed to perform analyses "of small signals in high-statistics neutrino oscillation experiments". It is used to generate the expected event distributions from several MC sets, which can then be compared to the observed data. The expectation for each set is calculated in parallel, applying physics and nuisance parameter effects in a stage-wise manner, before combining the final expectation from all the sets.

[35]: Aartsen et al. (2020), "Computational techniques for the analysis of small signals in high-statistics neutrino oscillation experiments"

3.2.2 Test Statistic

The measurements are performed by comparing the weighted MC to the data. Through variation of the nuisance and physics parameters that govern the weights, the best matching set of parameters can be found. The comparison is done using a modified χ^2 defined as

$$\chi^2_{\text{mod}} = \sum_{i \in \text{bins}} \frac{(N_i^{\text{exp}} - N_i^{\text{obs}})^2}{N_i^{\text{exp}} + (\sigma_i^{\nu})^2 + (\sigma_i^{\mu})^2 + (\sigma_i^{\text{HNL}})^2} + \sum_{j \in \text{syst}} \frac{(s_j - \hat{s}_j)^2}{\sigma_{s_j}^2}, \quad (3.1)$$

as the *test statistic (TS)*. The total even expectation is $N_i^{\text{exp}} = N_i^{\nu} + N_i^{\mu} + N_i^{\text{HNL}}$, where N_i^{ν} , N_i^{μ} , and N_i^{HNL} are the expected number of events in bin i from neutrinos, atmospheric muons, and HNLs, while N_i^{obs} is the observed number of events in bin i . The expected number of events from each particle type is calculated by summing the weights of all events in the bin $N_i^{\text{type}} = \sum_i^{\text{type}} \omega_i$, with the statistical uncertainty being $(\sigma_i^{\text{type}})^2 = \sum_i^{\text{type}} \omega_i^2$. The additional term in Equation 3.1 is included to apply a penalty term for prior knowledge of the systematic uncertainties of the parameters where they are known. s_j are the systematic parameters that are varied in the fit, while \hat{s}_j are their nominal values and σ_{s_j} are the known uncertainties.

Do I want/need to include the description of the KDE muon estimation?

Add table with all systematic uncertainties used in this analysis.

add final level effects of varying the axial mass parameters (or example of one)

add final level effects of varying the DIS parameter (or example of one)

3.2.3 Systematic Uncertainties

3.3 Analysis Checks

Fitting to data will be performed in a *blind* manner, where the analyzer does not immediately see the fitted physics and nuisance parameter values, but first checks that a set of pre-defined *goodness of fit (GOF)* criteria are fulfilled. If those criteria are met to satisfaction the fit results are unblinded and the full result can be revealed. Before these blind fits to data are run, the robustness of the analysis method is tested using pseudo-data that is generated using the MC sets.

3.3.1 Minimization Robustness

1: There is a degeneracy between the lower octant ($\theta_{23} < 45^\circ$) and the upper octant ($\theta_{23} > 45^\circ$), which can lead to TS minima (local and global) at two positions that are mirrored around 45° in θ_{23} .

[37]: Dembinski et al. (2022), *scikit-hep/minuit*: v2.17.0

[38]: James et al. (1975), “Minuit: A System for Function Minimization and Analysis of the Parameter Errors and Correlations”

Fit	Err.	Prec.	Tol.
Coarse	1e-1	1e-8	1e-1
Fine	1e-5	1e-14	1e-5

Table 3.4: Migrad settings for the two stages in the minimization routine. *Err.* are the step size for the numerical gradient estimation, *Prec.* is the precision with which the LLH is calculated, and *Tol.* is the tolerance for the minimization.

2: A pseudo-data set without statistical fluctuations is called Asimov data set.

Do I want additional plots for this (fit diff, LLH distr, minim. stats, param. fits)?

To find the set of parameters that describes the data best, a staged minimization routine is used. In the first stage, a fit with coarse minimizer settings is performed to find a rough estimate of the *best fit point* (*BFP*). In the second stage, the fit is performed again in both octants¹ of θ_{23} , starting from the BFP of the coarse fit. For each individual fit the *MIGRAD* routine of *IMINUIT* [37] is used to minimize the χ^2 TS defined in Equation 3.1. *Iminuit* is a fast, python compatible minimizer based on the *MINUIT2* C++ library [38]. The individual minimizer settings are shown in Table 3.4.

To test the minimization routine and to make sure it consistently recovers any injected physics parameters, pseudo-data sets are produced from the MC by choosing the nominal nuisance parameters and specific physics parameters, without adding any statistical or systematic fluctuations to it. These so-called *Asimov*² data sets are then fit back with the full analysis chain. This type of test is called *Asimov inject/recover test*. A set of mixing values between 10^{-3} and 10^0 is injected and fit back. Even though this range is well within the excluded regions by other experiments, discussed in Section 1.2.3, this covers the current sensitive region of the analysis in IceCube DeepCore. Without fluctuations the fit is expected to always recover the injected parameters (both physics and nuisance parameters). The fitted mixing values from the Asimov inject/recover tests are compared to the true injected values in Figure 3.1 for the 0.6 GeV set. As expected, the fit is always able to recover the injected physcis parameter and the nuisance paramters. Additional plots for the other mass sets can be found in Section B.1.

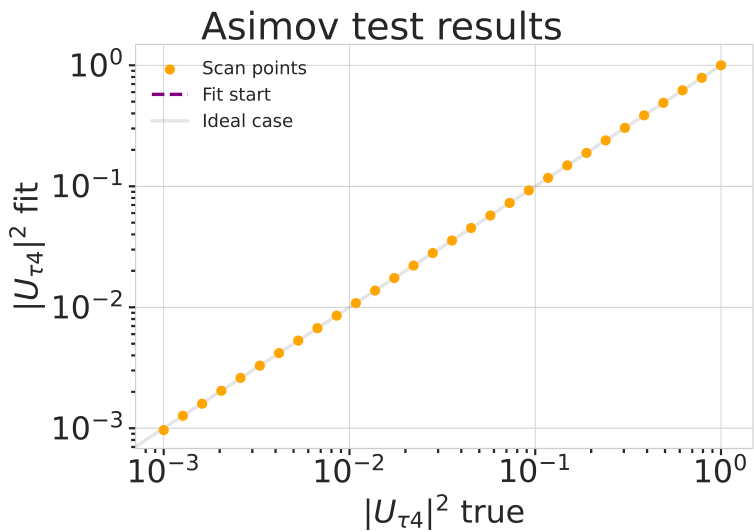
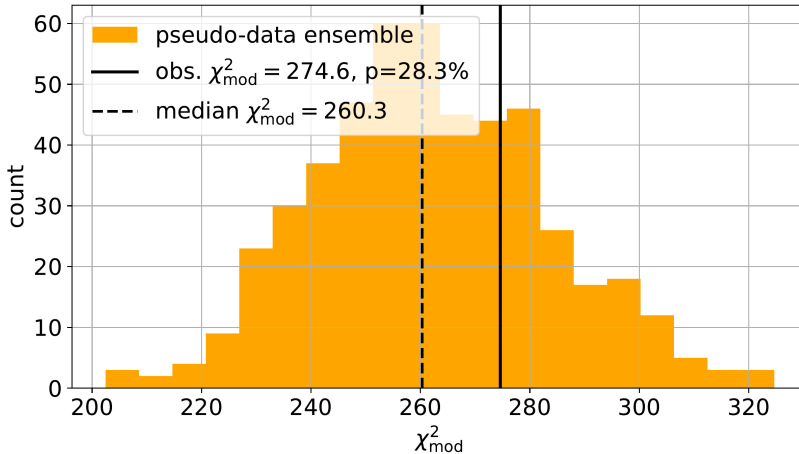


Figure 3.1: Asimov inject/recover test for the 0.6 GeV mass set. Mixing values between 10^{-3} and 10^0 are injected and fit back with the full analysis chain. The injected parameter is always recovered within the statistical uncertainty.

3.3.2 Ensemble Tests

To estimate the goodness of fit, pseudo-data is generated from the MC by injecting the BFP parameters as true parameters and then fluctuating the expected bin counts using Poisson fluctuation. The resulting pseudo-data sets are then fit back with the analysis chain. By comparing the

distribution of TS values from this *ensemble* of pseudo-data trials to the TS of the fit to real data, a p-value can be calculated. The p-value is the probability of finding a TS value at least as large as the one from the data fit. Figure 3.2 shows the TS distribution from the ensemble tests for the 0.6 GeV mass set and the observed TS value from the fit, resulting in a p-value of 28.5 %³. Plots for the addition two mass sets are shown in Section B.1.1.



Add bin-wise TS distribution? Add 3D TS maps?

3: The p-values for the 0.3 GeV and 1.0 GeV are 28.3 % and 26.0 %, respectively.

Figure 3.2: Observed fit TS and TS distribution from pseudo-data trials for the 0.6 GeV mass set.

3.4 Results

3.4.1 Best Fit Parameters

3.4.2 Upper Limits

3.4.3 Post-Fit Data/MC Agreement

3.4.4 Likelihood Coverage

Add table with BFP mixings and their uncertainties from scan assuming wilks?

Add table with BFP nuisance parameters and maybe a plot showing them compared to nominal?

APPENDIX

A

Heavy Neutral Lepton Signal Simulation

A.1 Model Independent Simulation Distributions

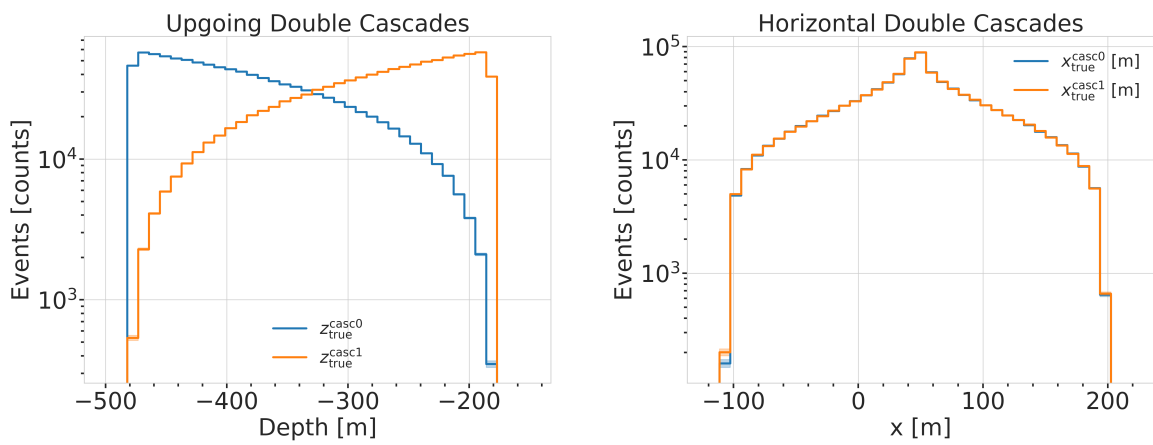


Figure A.1: Generation level distributions of the simplistic simulation sets. Vertical positions (left) and horizontal positions (right) of both sets are shown.

- Re-make plot with x,y for horizontal set one plot!
- Re-make plot with x, y, z for both cascades in one.
- Re-arrange plots in a more sensible way.

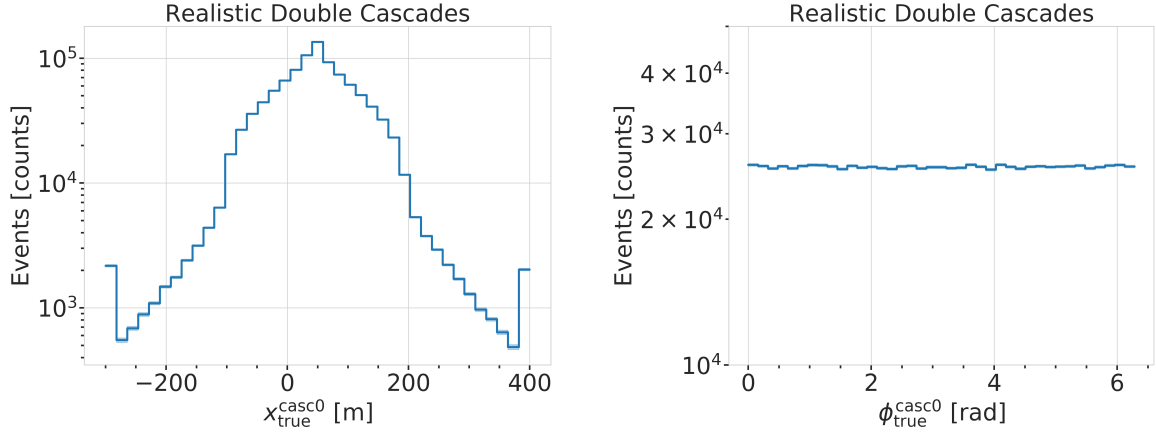


Figure A.2: Generation level distributions of the realistic simulation set. Shown are the cascade x, y, z positions (left) and direction angles (right).

A.2 Model Dependent Simulation Distributions

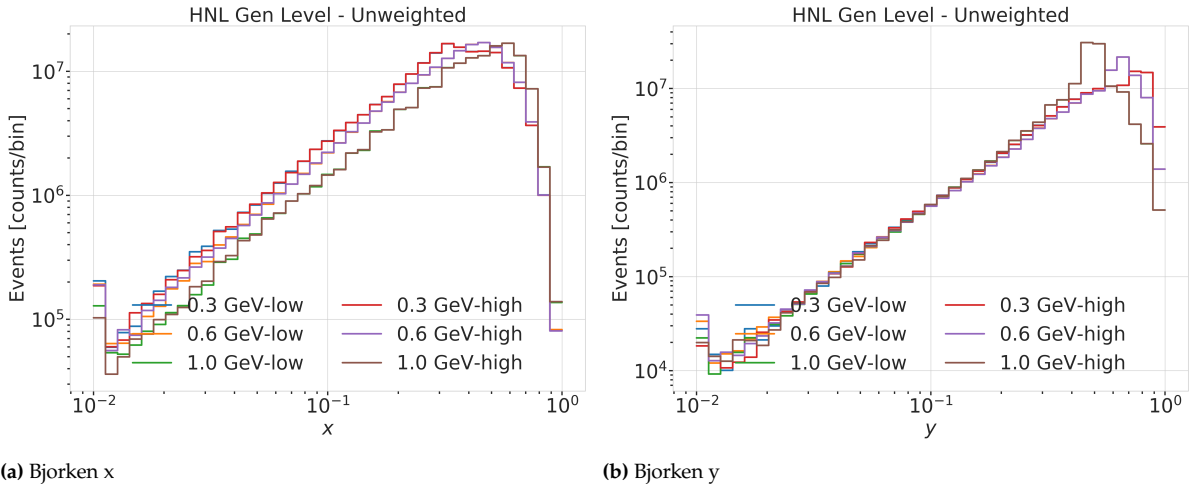


Figure A.3: Generation level distributions of the model dependent simulation.

B

Analysis Checks

B.1 Minimization Robustness

Figure B.1 shows additional Asimov inject/recover tests for the 0.3 GeV and the 1.0 GeV mass sets. The tests were described in Section 3.3.1.

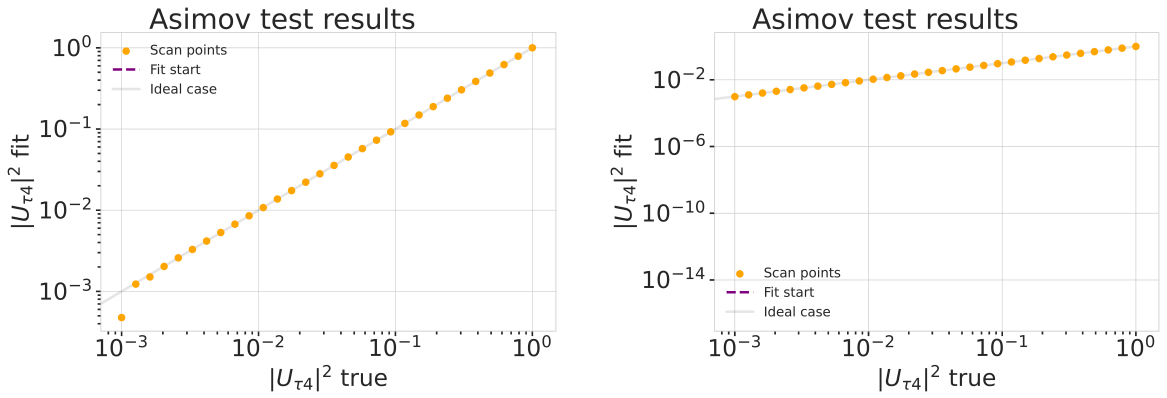


Figure B.1: Asimov inject/recover test for the 0.3 GeV (left) and the 1.0 GeV (right) mass sets. Mixing values between 10^{-3} and 10^0 are injected and fit back with the full analysis chain. The injected parameter is always recovered within the statistical uncertainty.

B.1.1 Ensemble Tests

Figure B.2 shows additional TS distributions from pseudo-data trials and the observed TS from the fit to the data for the ensemble for the 0.3 GeV and the 1.0 GeV mass sets. The tests were described in Section 3.3.2.

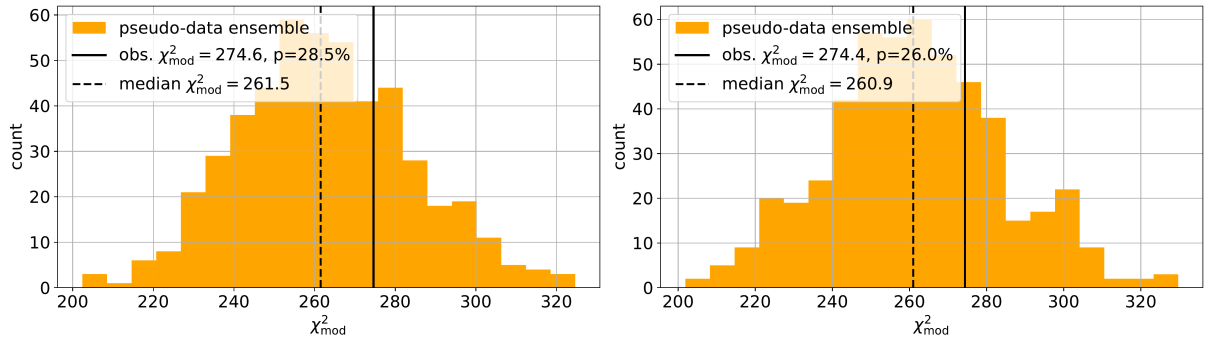


Figure B.2: Observed fit TS and TS distribution from pseudo-data trials for the 0.3 GeV (left) and the 1.0 GeV (right) mass set.

Bibliography

Here are the references in citation order.

- [1] C. N. Yang and R. L. Mills. "Conservation of Isotopic Spin and Isotopic Gauge Invariance". In: *Physical Review* 96.1 (Oct. 1954), pp. 191–195. doi: [10.1103/PhysRev.96.191](https://doi.org/10.1103/PhysRev.96.191) (cited on page 1).
- [2] S. Weinberg. "A Model of Leptons". In: *Phys. Rev. Lett.* 19 (21 Nov. 1967), pp. 1264–1266. doi: [10.1103/PhysRevLett.19.1264](https://doi.org/10.1103/PhysRevLett.19.1264) (cited on page 1).
- [3] S. L. Glashow. "Partial-symmetries of weak interactions". In: *Nuclear Physics* 22.4 (Feb. 1961), pp. 579–588. doi: [10.1016/0029-5582\(61\)90469-2](https://doi.org/10.1016/0029-5582(61)90469-2) (cited on page 1).
- [4] R. Jackiw. "Physical Formulations: Elementary Particle Theory. Relativistic Groups and Analyticity. Proceedings of the eighth Nobel Symposium, Aspenäsgården, Lerum, Sweden, May 1968. Nils Svartholm, Ed. Interscience (Wiley), New York, and Almqvist and Wiksell, Stockholm, 1969. 400 pp., illus. \$31.75." In: *Science* 168.3936 (1970), pp. 1196–1197. doi: [10.1126/science.168.3936.1196.b](https://doi.org/10.1126/science.168.3936.1196.b) (cited on page 1).
- [5] P. Higgs. "Broken symmetries, massless particles and gauge fields". In: *Physics Letters* 12.2 (1964), pp. 132–133. doi: [https://doi.org/10.1016/0031-9163\(64\)91136-9](https://doi.org/10.1016/0031-9163(64)91136-9) (cited on page 1).
- [6] M. Gell-Mann. "A Schematic Model of Baryons and Mesons". In: *Resonance* 24 (1964), pp. 923–925 (cited on page 1).
- [7] G. Zweig. "An SU(3) model for strong interaction symmetry and its breaking. Version 2". In: *DEVELOPMENTS IN THE QUARK THEORY OF HADRONS. VOL. 1. 1964 - 1978*. Ed. by D. B. Lichtenberg and S. P. Rosen. Feb. 1964, pp. 22–101 (cited on page 1).
- [8] D. J. Gross and F. Wilczek. "Ultraviolet Behavior of Non-Abelian Gauge Theories". In: *PRL* 30.26 (June 1973), pp. 1343–1346. doi: [10.1103/PhysRevLett.30.1343](https://doi.org/10.1103/PhysRevLett.30.1343) (cited on page 1).
- [9] C. Giunti and C. W. Kim. *Fundamentals of Neutrino Physics and Astrophysics*. Oxford University Press, Mar. 2007 (cited on page 1).
- [10] M. D. Schwartz. *Quantum Field Theory and the Standard Model*. Cambridge University Press, 2013 (cited on page 1).
- [11] A. Terliuk. "Measurement of atmospheric neutrino oscillations and search for sterile neutrino mixing with IceCube DeepCore". PhD thesis. Berlin, Germany: Humboldt-Universität zu Berlin, Mathematisch-Naturwissenschaftliche Fakultät, 2018. doi: [10.18452/19304](https://doi.org/10.18452/19304) (cited on pages 3, 8).
- [12] M. Thomson. *Modern particle physics*. Cambridge [u.a.]: Cambridge University Press, 2013, XVI, 554 S. (Cited on page 3).
- [13] R. Davis, D. S. Harmer, and K. C. Hoffman. "Search for Neutrinos from the Sun". In: *Phys. Rev. Lett.* 20 (21 May 1968), pp. 1205–1209. doi: [10.1103/PhysRevLett.20.1205](https://doi.org/10.1103/PhysRevLett.20.1205) (cited on page 4).
- [14] Y. Fukuda et al. "Evidence for Oscillation of Atmospheric Neutrinos". In: *Phys. Rev. Lett.* 81 (8 Aug. 1998), pp. 1562–1567. doi: [10.1103/PhysRevLett.81.1562](https://doi.org/10.1103/PhysRevLett.81.1562) (cited on page 4).
- [15] Q. R. Ahmad and other. "Direct Evidence for Neutrino Flavor Transformation from Neutral-Current Interactions in the Sudbury Neutrino Observatory". In: *Phys. Rev. Lett.* 89 (1 June 2002), p. 011301. doi: [10.1103/PhysRevLett.89.011301](https://doi.org/10.1103/PhysRevLett.89.011301) (cited on page 4).
- [16] M. Tanabashi et al. "Review of Particle Physics". In: *Phys. Rev. D* 98 (3 Aug. 2018), p. 030001. doi: [10.1103/PhysRevD.98.030001](https://doi.org/10.1103/PhysRevD.98.030001) (cited on pages 4, 6, 9).
- [17] M. Aker et al. "Direct neutrino-mass measurement with sub-electronvolt sensitivity". In: *Nature Phys.* 18.2 (2022), pp. 160–166. doi: [10.1038/s41567-021-01463-1](https://doi.org/10.1038/s41567-021-01463-1) (cited on page 4).

- [18] S. Alam et al. "Completed SDSS-IV extended Baryon Oscillation Spectroscopic Survey: Cosmological implications from two decades of spectroscopic surveys at the Apache Point Observatory". In: *Phys. Rev. D* 103 (8 Apr. 2021), p. 083533. doi: [10.1103/PhysRevD.103.083533](https://doi.org/10.1103/PhysRevD.103.083533) (cited on page 4).
- [19] N. Aghanim et al. "Planck2018 results: VI. Cosmological parameters". In: *Astronomy & Astrophysics* 641 (Sept. 2020), A6. doi: [10.1051/0004-6361/201833910](https://doi.org/10.1051/0004-6361/201833910) (cited on page 4).
- [20] P. Coloma et al. "GeV-scale neutrinos: interactions with mesons and DUNE sensitivity". In: *Eur. Phys. J. C* 81.1 (2021), p. 78. doi: [10.1140/epjc/s10052-021-08861-y](https://doi.org/10.1140/epjc/s10052-021-08861-y) (cited on pages 6, 11, 13).
- [21] M. Honda et al. "Atmospheric neutrino flux calculation using the NRLMSISE-00 atmospheric model". In: *Phys. Rev. D* 92 (2 July 2015), p. 023004. doi: [10.1103/PhysRevD.92.023004](https://doi.org/10.1103/PhysRevD.92.023004) (cited on page 7).
- [22] A. Fedynitch et al. "Calculation of conventional and prompt lepton fluxes at very high energy". In: *European Physical Journal Web of Conferences*. Vol. 99. European Physical Journal Web of Conferences. Aug. 2015, p. 08001. doi: [10.1051/epjconf/20159908001](https://doi.org/10.1051/epjconf/20159908001) (cited on page 7).
- [23] J. A. Formaggio and G. P. Zeller. "From eV to EeV: Neutrino cross sections across energy scales". In: *Rev. Mod. Phys.* 84 (3 Sept. 2012), pp. 1307–1341. doi: [10.1103/RevModPhys.84.1307](https://doi.org/10.1103/RevModPhys.84.1307) (cited on page 9).
- [24] S. Bilenky and B. Pontecorvo. "Lepton mixing and neutrino oscillations". In: *Physics Reports* 41.4 (1978), pp. 225–261. doi: [10.1016/0370-1573\(78\)90095-9](https://doi.org/10.1016/0370-1573(78)90095-9) (cited on page 8).
- [25] P. A. M. Dirac. "The Quantum Theory of the Emission and Absorption of Radiation". In: *Proceedings of the Royal Society of London Series A* 114.767 (Mar. 1927), pp. 243–265. doi: [10.1098/rspa.1927.0039](https://doi.org/10.1098/rspa.1927.0039) (cited on page 9).
- [26] T. Yanagida. "Horizontal Symmetry and Masses of Neutrinos". In: *Progress of Theoretical Physics* 64.3 (Sept. 1980), pp. 1103–1105. doi: [PTP.64.1103](https://doi.org/10.1143/PTP.64.1103) (cited on page 10).
- [27] P. Astier et al. "Search for heavy neutrinos mixing with tau neutrinos". In: *Phys. Lett. B* 506 (2001), pp. 27–38. doi: [10.1016/S0370-2693\(01\)00362-8](https://doi.org/10.1016/S0370-2693(01)00362-8) (cited on page 11).
- [28] R. Acciari et al. "New Constraints on Tau-Coupled Heavy Neutral Leptons with Masses mN=280–970 MeV". In: *Phys. Rev. Lett.* 127.12 (2021), p. 121801. doi: [10.1103/PhysRevLett.127.121801](https://doi.org/10.1103/PhysRevLett.127.121801) (cited on page 11).
- [29] J. Orloff, A. N. Rozanov, and C. Santoni. "Limits on the mixing of tau neutrino to heavy neutrinos". In: *Phys. Lett. B* 550 (2002), pp. 8–15. doi: [10.1016/S0370-2693\(02\)02769-7](https://doi.org/10.1016/S0370-2693(02)02769-7) (cited on page 11).
- [30] I. Boiarska et al. "Blast from the past: constraints from the CHARM experiment on Heavy Neutral Leptons with tau mixing". In: (July 2021) (cited on page 11).
- [31] P. Abreu et al. "Search for neutral heavy leptons produced in Z decays". In: *Z. Phys. C* 74 (1997). [Erratum: *Z.Phys.C* 75, 580 (1997)], pp. 57–71. doi: [10.1007/s002880050370](https://doi.org/10.1007/s002880050370) (cited on page 11).
- [32] P. Coloma et al. "Double-Cascade Events from New Physics in Icecube". In: *Phys. Rev. Lett.* 119.20 (2017), p. 201804. doi: [10.1103/PhysRevLett.119.201804](https://doi.org/10.1103/PhysRevLett.119.201804) (cited on pages 10, 11).
- [33] P. Coloma. "Icecube/DeepCore tests for novel explanations of the MiniBooNE anomaly". In: *Eur. Phys. J. C* 79.9 (2019), p. 748. doi: [10.1140/epjc/s10052-019-7256-8](https://doi.org/10.1140/epjc/s10052-019-7256-8) (cited on page 11).
- [34] S. Yu and J. Micallef. "Recent neutrino oscillation result with the IceCube experiment". In: *38th International Cosmic Ray Conference*. July 2023 (cited on page 22).
- [35] M. G. Aartsen et al. "Computational techniques for the analysis of small signals in high-statistics neutrino oscillation experiments". In: *Nucl. Instrum. Meth. A* 977 (2020), p. 164332. doi: [10.1016/j.nima.2020.164332](https://doi.org/10.1016/j.nima.2020.164332) (cited on page 23).
- [36] I. Collaboration. <https://github.com/icecube/pisa> (cited on page 23).
- [37] H. Dembinski et al. *scikit-hep/minuit*: v2.17.0. Version v2.17.0. Sept. 2022. doi: [10.5281/zenodo.7115916](https://doi.org/10.5281/zenodo.7115916) (cited on page 24).
- [38] F. James and M. Roos. "Minuit: A System for Function Minimization and Analysis of the Parameter Errors and Correlations". In: *Comput. Phys. Commun.* 10 (1975), pp. 343–367. doi: [10.1016/0010-4655\(75\)90039-9](https://doi.org/10.1016/0010-4655(75)90039-9) (cited on page 24).